Exploring Burstein-Moss Type Effect in Nickel Doped Hematite Dendrite Nanostructure for Enhanced Photo-electrochemical Water Splitting

Soniya Gahlawat, Jaspreet Singh, Ashok Kumar Yadav Pravin P. Ingole*

[1]Department of Chemistry, Indian Institute of Technology Delhi, New Delhi, India 110016.
[2]Technical Physics Devision, Raja Ramanna Centre for Advanced Technology (RRCAT), Indore, India.
[3]Atomic & Molecular Physics Devision, Raja Ramanna Centre for Advanced Technology (RRCAT), Indore, India.
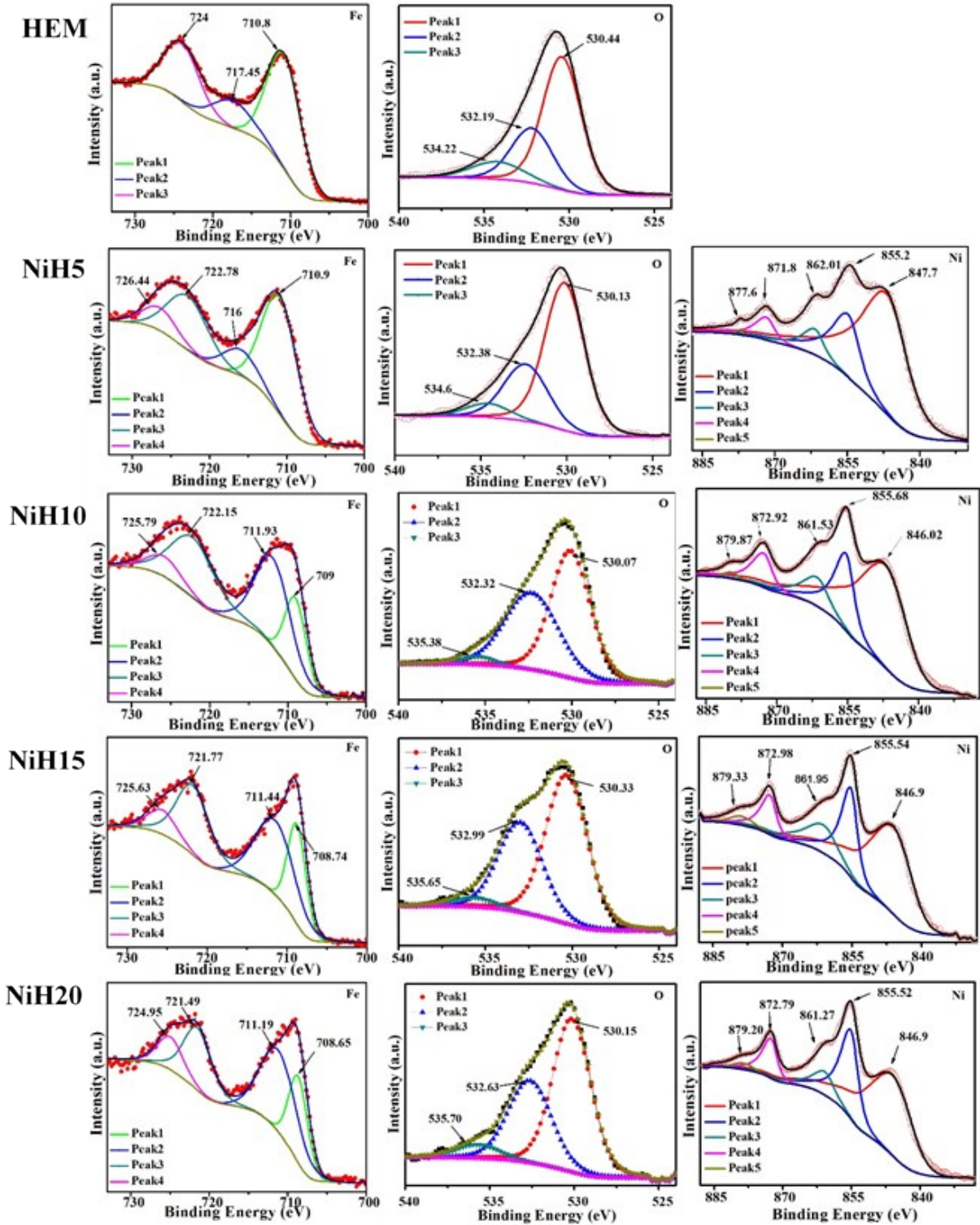
Supporting Information

Fig: SI-1 HAXPES Spectra of Pure hematite and $Ni_xFe_{2-x}O_3$ nanocomposites for Fe, O and Ni element respectively.
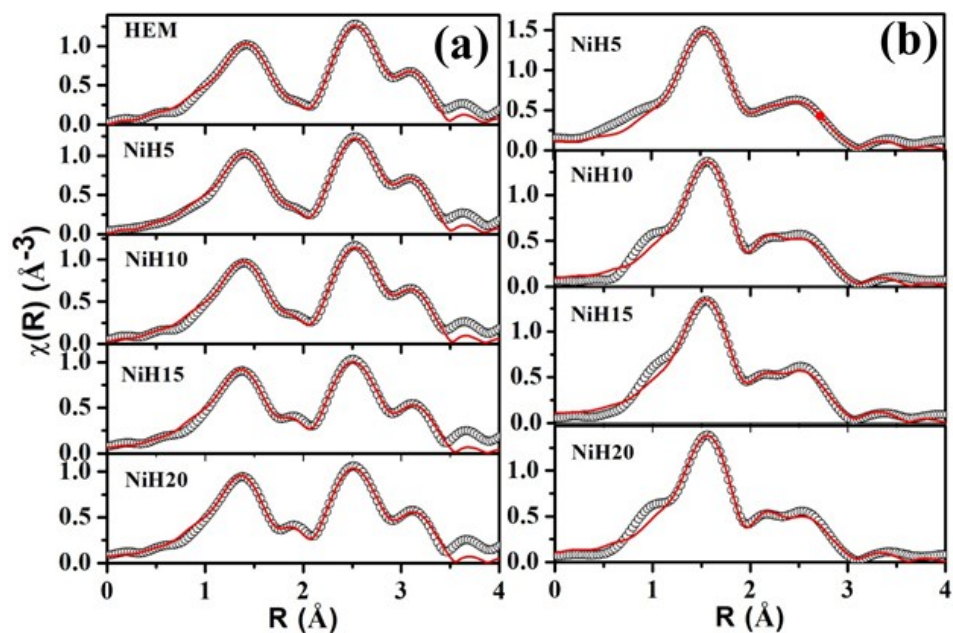
Fig. SI-2: Fourier transformed EXAFS spectra of pure hematite and $Ni_xFe_{2-x}O_3$ nanocomposites at (a) Fe K edge (b) Ni K edge respectively. The experimental spectra are represented by Scatter points and theoretical fit is represented by Solid line.

Table SI-1: Bond length, coordination number and disorder factor obtain by EXAFS fitting at Fe K-edge. The Fe-Fe coordination is kept constant during the fitting.

Path	Parameters	Hematite	NiH5	NiH10	NiH15	NiH20
Fe-O	R (Å)	1.91±0.01	1.90±0.01	1.90±0.01	1.89±0.01	1.89±0.01
	N	2.97±0.10	3.07±0.12	3.21±0.15	3.38±0.18	3.41±0.18
	σ^2	0.0066±0.0008	0.0060±0.0012	0.0069±0.0014	0.0072±0.0017	0.0068±0.0017
Fe-O	R (Å)	2.05±0.01	2.06±0.01	2.07±0.01	2.09±0.01	2.09±0.01
	N	2.97±0.10	3.07±0.12	3.21±0.15	3.38±0.18	3.41±0.18
	σ^2	0.0111±0.000	0.0104±0.001	0.0122±0.001	0.0122±0.001	0.0124±0.001

		5	0	1	4	3
Fe-Fe	R (Å)	2.90±0.01	2.90±0.01	2.90±0.01	2.90±0.01	2.90±0.01
	N	3	3	3	3	3
	σ^2	0.0046±0.0003	0.0052±0.0006	0.0063±0.0006	0.0083±0.0009	0.008±0.0008
Fe-Fe	R (Å)	3.38±0.02	3.37±0.01	3.37±0.01	3.37±0.01	3.37±0.01
	N	3	3	3	3	3
	σ^2	0.0013±0.0006	0.0017±0.0006	0.0027±0.0006	0.0050±0.0010	0.0049±0.0010

Table SI-2: Bond length, coordination number and disorder factor obtain by EXAFS fitting at U L3 edge.

Path	Parameters	NiH5	NiH10	NiH15	NiH20
Ni-O	R (Å)	1.96±0.01	1.97±0.01	1.96±0.01	1.96±0.01
	N	3.11±0.06	2.74±0.08	3.04±0.15	2.85±0.11
	σ^2	0.001±0.0005	0.0019±0.0008	0.0027±0.0011	0.0029±0.0009
Ni-O	R (Å)	2.10±0.01	2.08±0.01	2.09±0.01	2.07±0.01
	N	3.11±0.06	2.74±0.08	3.04±0.15	2.85±0.11
	σ^2	0.0011±0.0005	0.0019±0.0008	0.0038±0.0011	0.0024±0.0008
Ni-Fe/Ni	R (Å)	2.86±0.01	2.84±0.01	2.85±0.01	2.83±0.02
	N	3.26±0.07	2.89±0.09	3.19±0.17	2.99±0.12
	σ^2	0.0185±0.0014	0.0173±0.0022	0.0191±0.0031	0.0204±0.0029

Ni-Fe/Ni	R (Å)	3.45±0.01	3.44±0.01	3.44±0.01	3.42±0.01
	N	3.26±0.07	2.89±0.09	3.19±0.17	2.99±0.12
	σ^2	0.0174±0.0021	0.0163±0.0032	0.0149±0.0034	0.0156±0.0029

Elemental mapping analysis was done by recording EDAX spectra using Hitachi tabletop microscope (Model: TM 3000 equipped with SwiftED3000 SDD detector) at an accelerating voltage of 15 kV.
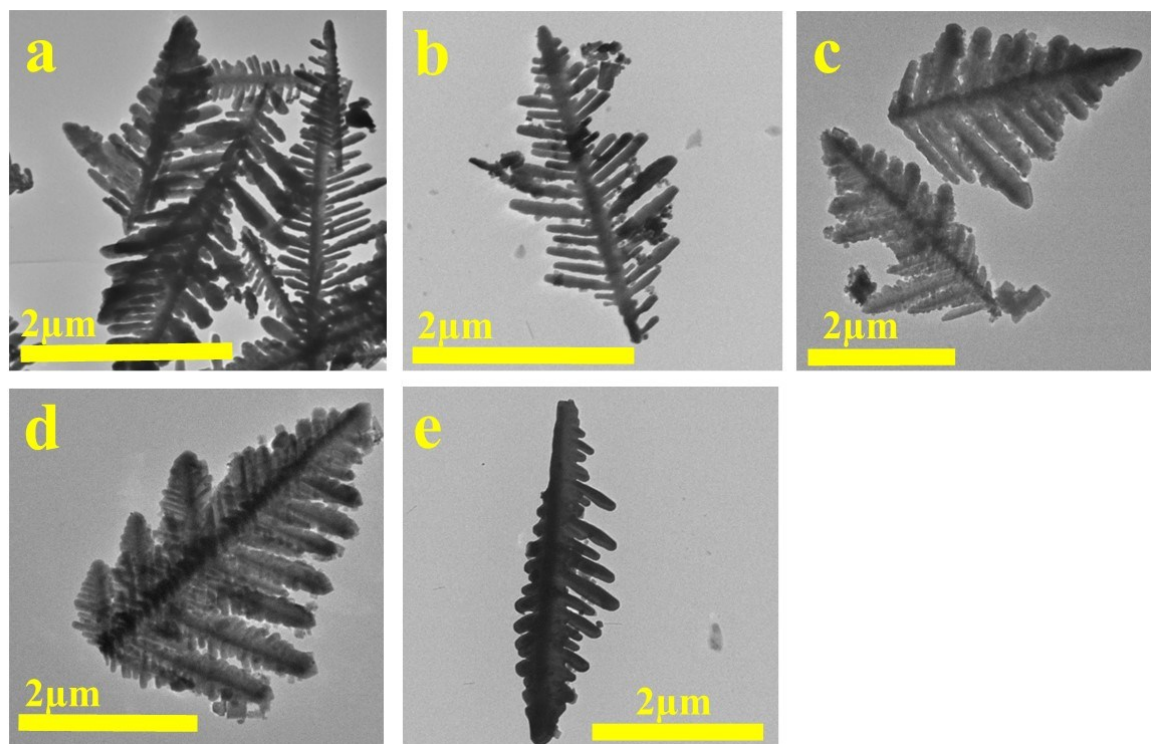

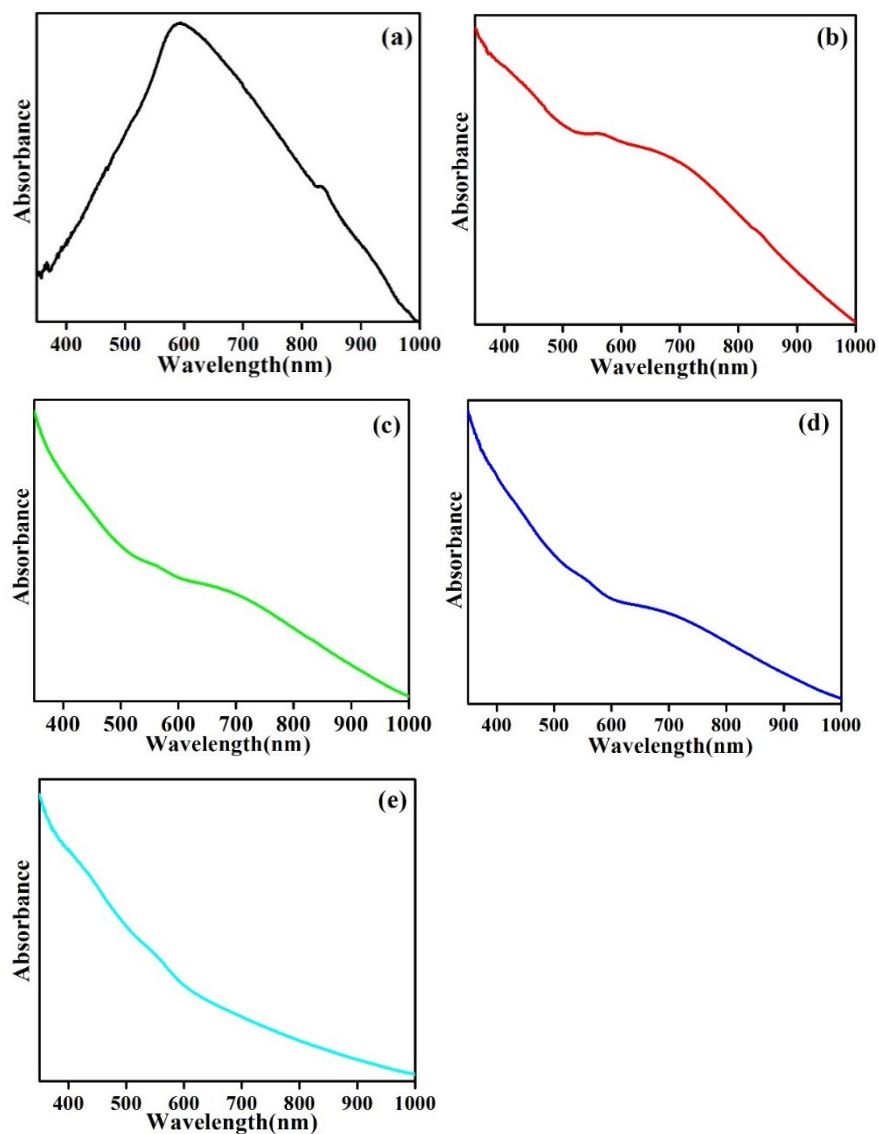*Fig. SI-3. TEM image of (a) Hem (b) NiH5 (c) NiH10 (d) NiH15 (e) NiH20.*

Fig SI-4 UV-Vis spectra of un-doped hematite and $Ni_xFe_{2-x}O_3$ nanocomposites (a) Hem (b) NiH5 (c) NiH10 (d) NiH15 (e) NiH20.

From Fig. SI-4, it is clear that hematite gives absorption at 599 nm. After doping absorption peak was not as pronounced as in un-doped hematite. For NiH5 a peak at 577 was observed. For NiH10, NiH15 and NiH20 peak was observed at 575, 569, 565 nm, respectively. Also, in all doped samples a shoulder was observed in 600 to 800 nm region.
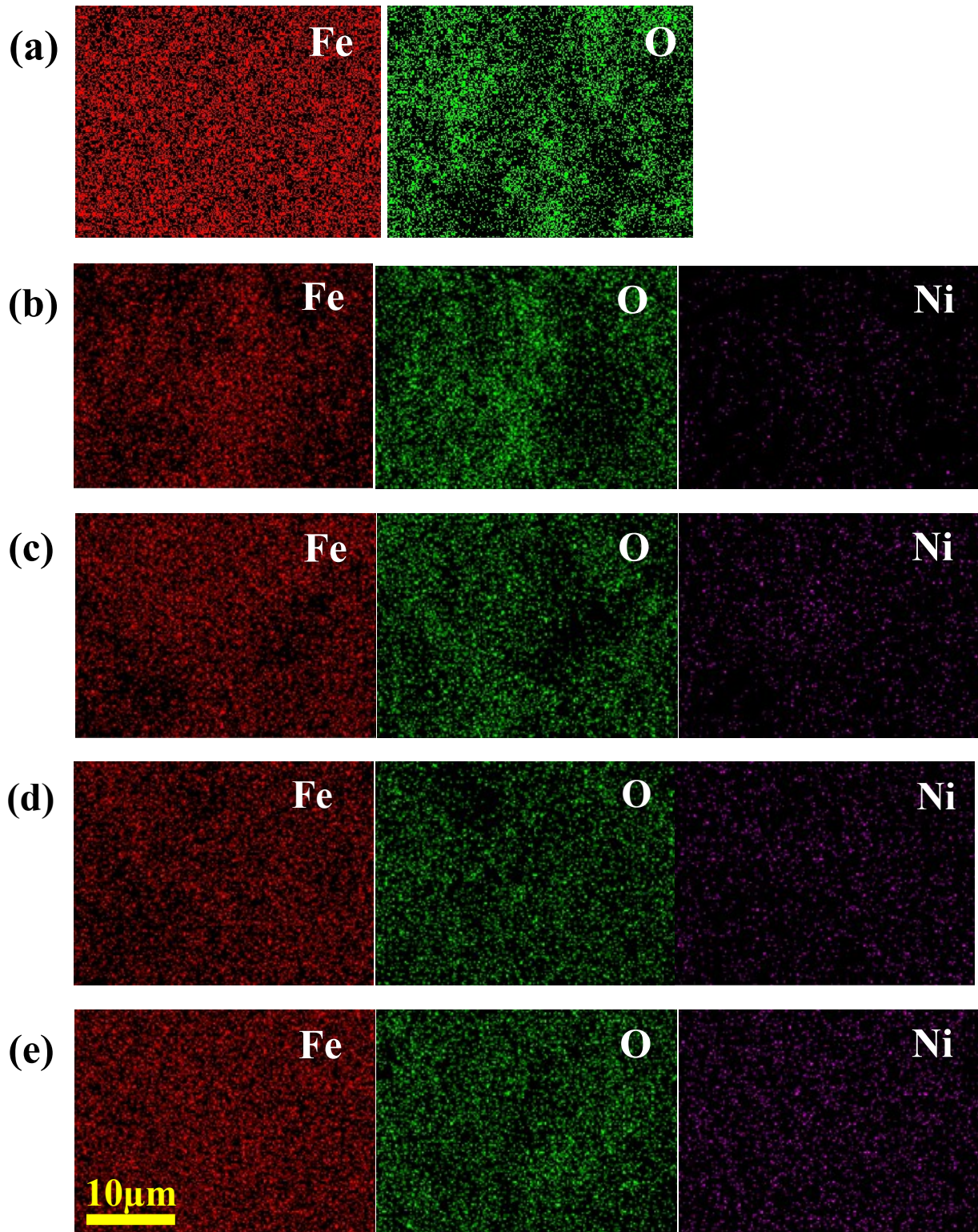
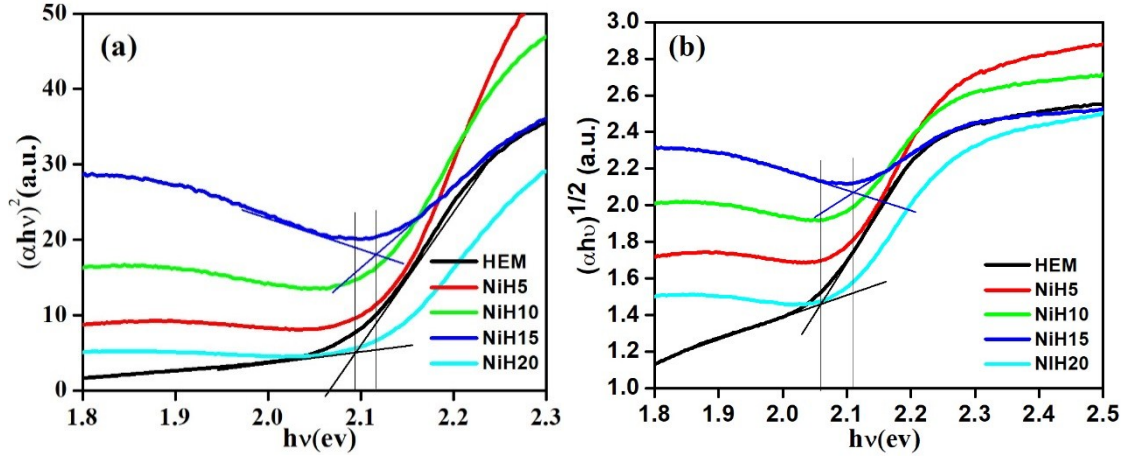*Fig. SI-5 Elemental mapping images of (a) Hem (b) NiH5 (c) NiH10 (d) NiH15 (e) NiH20.*

Fig. SI-6. Kubelka-Munk plot of hematite and other doped sample (a) for direct transition (b) for indirect transition derived from DRS spectra.
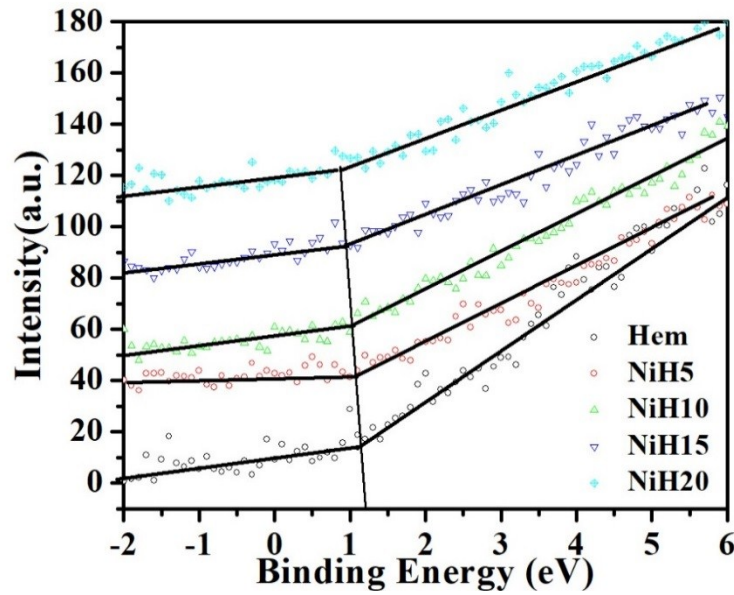

Fig. SI-7. VBXPS Spectra of Pure hematite and $Ni_xFe_{2-x}O_3$ nanocomposites samples.

Valence band maxima of un-doped hematite and $Ni_xFe_{2-x}O_3$ nanocomposites was determined by extrapolation of linear part of low energy edge of VB [1]. Energy of valence band maxima for hematite was 1.12 and 1.04, 1.01, 0.92, 0.87 for NiH5, NiH10, NiH15, NiH20 resp. relative to Fermi energy level (E_F). The work function ($W_S = E_F - E_{VAC}$) for hematite is 5.4 eV [2]. Finally, VBM values are converted vs. NHE as shown in table SI-3 [1] and also tabulated in Table 2 of the manuscript. Conduction band edge (CBE) was determined using optical band gap and VBM.

Table SI-3: Conversion of valence band maxima values to NHE scale.

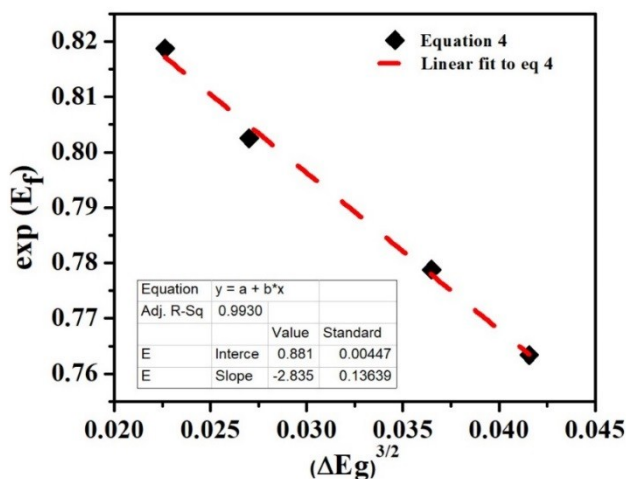| Sample	VBM w.r.t E_F (eV)	VBM vs. NHE (eV)
HEM	1.12 ± 0.03	1.12-4.5+5.4 = 2.02
NiH5	1.04 ± 0.03	1.04-4.5+5.4 = 1.94
NiH10	1.01 ± 0.03	1.01-4.5+5.4 = 1.91
NiH15	0.92 ± 0.03	0.92-4.5+5.4 = 1.82
NiH20	0.87 ± 0.03	0.87-4.5+5.4 = 1.77

Fig. SI-8 Variation of $(\Delta E_g)^{3/2}$ versus exponential of Fermi level (E_F) in a linear fashion suggest that the band gap widening after doping is due to only Burstein-Moss effect.
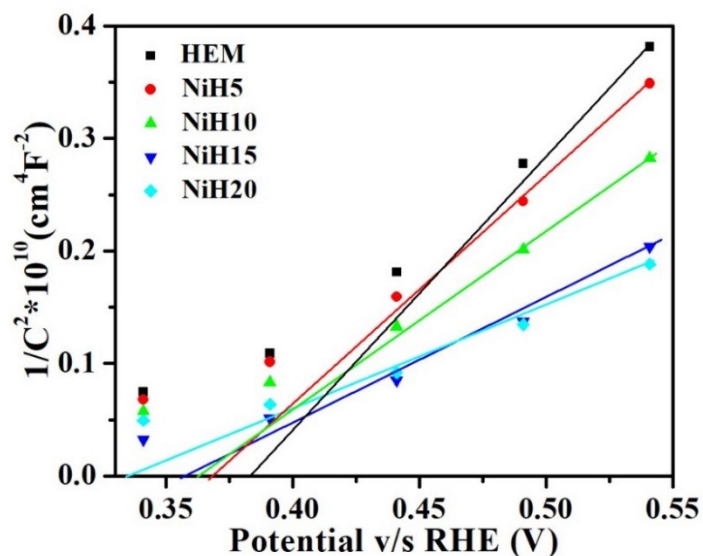

Fig. SI-9. Zoomed image of Mott-Schottky Plot indicating Flat band potential value.

Table SI-4. Circuits used simulation of impedance curves, various resistances obtained after simulations, exchange current density and rate constant.

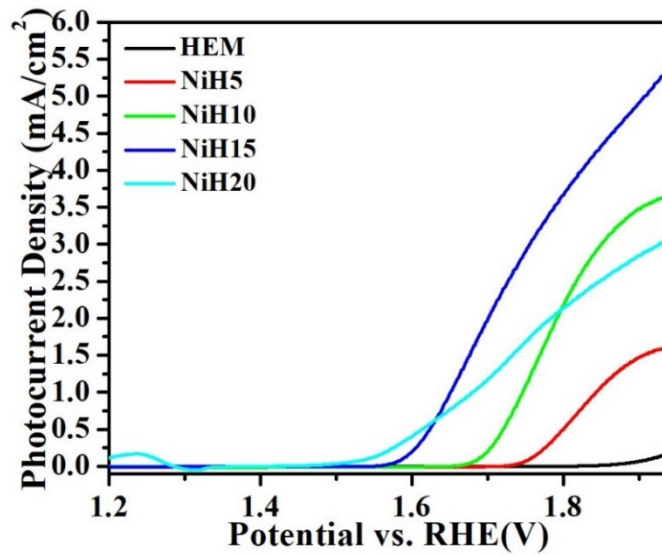| Sample	Circuit	$R_1(\Omega)$	$R_2(\Omega)$	$R_3(\Omega)$	j_o (A/cm^2)	k_o (cm/s)
Hem	R(Q(R(Q(RW))))	14.82	3.7×10^4	-	2.142×10^{-7}	6.25×10^{-9}
NiH5	R(C(R(C(RW))))	19.56	383	-	1.693×10^{-5}	4.39×10^{-7}
NiH10	R(C(R(C(RW))))(CR)	23.08	117	3.33	5.54×10^{-5}	1.44×10^{-6}
NiH15	R(C(R(Q(RW))))(C(RW))	12.8	50.9	0.14	1.274×10^{-4}	3.30×10^{-6}
NiH20	R(C(R(C(RW))))(CR)	107.4	71.3	25.3	7.44×10^{-5}	1.93×10^{-6}

Fig. SI-10. Photocurrent Response (light-dark) of pure hematite and $Ni_xFe_{2-x}O_3$ nanocomposites.
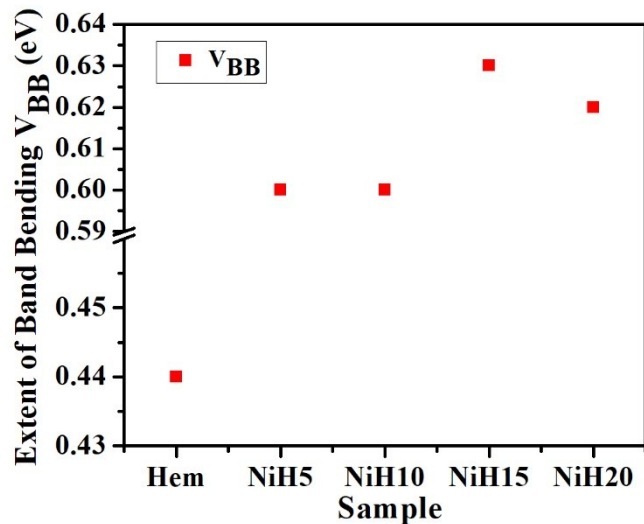
Fig. SI-11. The band bending potential for un-doped HDN and Ni$_x$Fe$_{2-x}$O$_3$ nanocomposites samples.

References:

1. Tian, Y.; Chang, B.; Yang, Z.; Zhou, B.; Xi, F.; Dong. X.; Graphitic Carbon Nitride-BiVO4 Heterojunctions: Simple Hydrothermal Synthesis and High Photocatalytic Performances. *Rsc. Adv.,* **2014**, 4, 4187–4193.
2. Kraushofer, F.; Jakub, Z.; Bichler, M.; Hulva, J.; Drmota, P.; Weinold, M.; Schmid, M.; Setvin, M.; Diebold, U.; Blaha, P.; Parkinson, G.S.; Atomic-Scale Structure of the Hematite α-Fe2O3(1$\bar{1}$02) "R-Cut" Surface, *J. Phys. Chem. C,* **2018**, *122*, 1657−1669.